

APPLICATION OF THE SLOPE DIFFRACTION METHOD FOR URBAN MICROWAVE PROPAGATION PREDICTION

K. Rizk⁺, R. Valenzuela^{*}, D. Chizhik^{*} and F. Gardiol⁺

⁺LEMA, Swiss Federal Institute of Technology, 1015 Lausanne, Switzerland, rizk@lema.epfl.ch

^{*}Bell Laboratories, Wireless Communications Res. Dept., POB 400, Holmdel NJ 07733, USA, rav@research.bell-labs.com

Abstract—This paper describes an algorithm for the implementation of the slope diffraction method [Andersen97] for an arbitrary configuration including edges or wedges. Validations against several published results are presented. The validations include examples of wedge configurations for which no validation of the slope diffraction method is available in the literature. Furthermore, an estimation for an urban environment of the gain in accuracy due to the use of the slope diffraction method over the classical Uniform Theory of Diffraction (UTD) was performed. It was found that the gain in accuracy is directly related to a factor we called the Transition Region Width TRW. TRW depends on the three parameters (the frequency freq, the separation between two screens d, the difference in building heights Δh) to give a single parameter: $\Delta h^2/(\lambda*d)$. It was shown that the classical UTD used with power summing of the rays can be accurate in configurations in which it was usually not considered to be valid. The results were obtained from 25 realizations of 10 equally spaced screens with heights distributed according to a uniform distribution U[18-Δh, 18+Δh] m.

I. INTRODUCTION

The assumption that propagation occurs in the vertical plane was successfully used for the prediction of propagation in urban and suburban macrocellular environments [Walfish88, Saunders91, Maciel93, Kurner93, Grosskopf94] and more recently for small cells (radius < 2 km) [Lachat97, Li97]. In vertical plane propagation, multiple diffractions by successive edges is the dominant mechanism. Among the several approaches to compute this mechanism the slope diffraction method [Andersen97] can handle any type of diffracting obstacle (wedge, knife edge or rounded surface) even in the transition region with, in general, a higher accuracy than the classical Uniform Theory of Diffraction (UTD). While it is more involved than the classical UTD it requires less computing time than Vogler's [Vogler82] approach.

In [Andersen97] few details were given on how to generalize the method for an arbitrary configuration including edges or wedges at unequal heights. In addition, no validation was available for wedge configurations. Multiple diffraction by wedges deserves particular attention as Andersen's method is among few schemes available in the literature that can handle multiple diffraction in transition region by wedges. This paper describes an algorithm for the implementation of the slope diffraction method for an arbitrary configuration including edges or wedges. Validations for wedge and edge configurations against several published results are presented. Furthermore, an estimation for an urban

environment of the amount of improvement due to the use of the slope diffraction method over the classical UTD was performed.

Sect. II describes an algorithm to implement the slope diffraction method for an arbitrary configuration including edges or wedges. Validations against several published results are presented in sect. III. Sect IV gives an estimate of the amount of improvement obtained due to the use of the slope diffraction method in comparison with the classical UTD in an urban environment. The conclusions are presented in sect.V.

II. IMPLEMENTATION OF THE SLOPE DIFFRACTION METHOD

This section presents an algorithm aimed at implementing Andersen's method in a computer program (for propagation prediction for instance) in an easier way than the one based on the explanation given in [Andersen97]. Thus Bach Andersen's method is brought a step closer to a computer implementation for the general case of wedges and edges with arbitrary heights.

Consider the scenario shown in Figure 1. The following discussion applies not only to wedges but to any type of diffracting object, provided that the diffraction coefficient of the object is known.

If $E_0|_{s_0=1}$ is the field at 1m from the transmitter, then the usual UTD computations lead to the following:

$$E_0(W_1) = \frac{E_0|_{s_0=1}}{s_0}$$

$$E_1(W_2) = E_0(W_1) D_1(W_2) A_1(s_1)$$

$$E_2(Rx) = E_1(W_2) D_2(Rx) A_2(s_2)$$

where:

$E_0(P)$ denotes the incident field emanating from Tx computed at a point P; $E_i(P)$ denotes the diffracted field by wedge i, $i=1,2$, computed at a point P; W_i denotes the location in the space of the vertex of the wedge i, $i=1,2$; $D_i(P)$ denotes the diffraction coefficient of wedge i, $i=1,2$, computed at a point P; A_i denotes the spreading factor of wedge i, $i=1,2$. $A_i(x) =$

$$\sqrt{\frac{\sum_{k=0}^{i-1} s_k}{\sum_{k=0}^{i-1} s_k + x}}$$

If the slope diffraction is taken into account, the above equations become:

$$E_I(W_2) = E_0(W_1) D_I(W_2) A_I(s_1)$$

$$E_2(Rx) = [E_I(W_2) D_2(Rx) + \frac{\partial E_I(W_2)}{\partial n} D_2^s(Rx)] A_2(s_2)$$

$$= [E_I(W_2) D_2(Rx) - \frac{\partial E_I(W_2)}{s_1 \partial \phi_1} D_2^s(Rx)] A_2(s_2)$$

$$= [E_I(W_2) D_2(Rx) - \frac{E_0}{s_0} \frac{\partial D_1(W_2)}{s_1 \partial \phi_1} D_2^s(Rx) A_I(s_1)] A_2(s_2) \quad (1)$$

where: $D_i^s(P)$ denotes the slope diffraction coefficient of wedge i , $i=1,2$, computed at a point P .

Thus on W_2 : the incident field is multiplied by D_2 AND the normal derivative of the incident field is multiplied by D_2^s . Thus two waves are generated on W_2 : an amplitude wave and a slope wave. In cases where there is a third wedge W_3 , the sum of the two waves generated at W_2 is multiplied by D_3 AND the normal derivative of the sum of the two waves generated at W_2 is multiplied by D_3^s .

Remaining to be determined are the values of the distance factors L and L_s , which appear in the expression of the diffraction coefficient and the slope diffraction coefficient respectively. The contribution of J. B. Andersen's [Andersen97] method is the criterion under which L and L_s are computed: L and L_s must be chosen to ensure that the diffracted field and its slope are continuous around the shadow boundaries of all wedges. L and L_s were calculated in [Andersen97] for an example of two screens located at the same height. The generalization relative to an arbitrary configuration did not make it clear how to compute L and L_s -values. Therefore we thought it would be of interest to give some details on our general implementation of the slope diffraction method. In the following it will be focused on the determination of L and L_s for arbitrary height configurations.

In Figure 1 the Shadow Boundary Points labeled as $SBP_{1,1}$ $SBP_{1,2}$ $SBP_{2,1}$ are the points that lie on the shadow boundary of successive wedges, and which are separated by the same distances as the wedges, i. e., s_1, s_2, \dots, s_n . To a wedge i correspond $(n-i+1)$ SB points, where n is the total number of wedges. The shadow boundary points are needed in our algorithm to determine the distance factors L and L_s for arbitrary configurations. Writing the appropriate continuity equation of all the waves incident on the shadow boundary points will determine the distance factors L and L_s . Since L and L_s depend only on the distance s_1, s_2, \dots, s_n , the L and L_s values determined at the SB points can be used to calculate both amplitude and slope diffraction of the wave incident on the wedge associated with the SB point in consideration.

Will follow an application of the above mentioned algorithm to the example shown in Figure 1:

a) The continuity equation for the amplitude wave emanating from Tx and reaching $SBP_{1,1}$ is:

$$0.5|E_0(SBP_{1,1})| = |E_I(SBP_{1,1})| \quad (2.a)$$

$$0.5|E_0(SBP_{1,1})| = |E_0(W_1) D_I(SBP_{1,1})| A_I(s_1) \quad (2.b)$$

$$|E_0(SBP_{1,1})| = |E_0(W_1)| \sqrt{L_{1,1}} A_I(s_1) \quad (2.c)$$

where: $L_{i,k}$ is the distance factor used to compute the diffraction from wedge i to $SBP_{i,k}$

Equ. (2) expresses the fact that at the shadow boundary the diffracted field ($E_I(SBP_{1,1})$) is one half the incident field ($E_0(SBP_{1,1})$). $L_{1,1}$ can easily be determined from (2). The substitution in Equ. (2.c) of $|D_I(SBP_{1,1})|$ by $0.5\sqrt{L_{1,1}}$ was explained in the case of an absorbing edge in [Andersen97]. This substitution holds also for a conducting knife edge or for the more general case of an impedance wedge. In fact, for the latter configuration it can be shown (see equ. 4.105 in [McNamara90]) that at the shadow boundary, the rapidly varying and discontinuous term in the diffraction coefficient reduces to the term for an absorbing edge.

It will be explained later why in equ. 2, (and below in 3 and 4) continuity was limited to the absolute values.

Writing a similar equation to (2) at $SBP_{1,2}$ allows determination of $L_{1,2}$. Obviously here $L_{1,1}$ and $L_{1,2}$ can be calculated from the analytical formula for the distance factor of a single diffraction, i.

$$e., \quad L_{1,1} = \frac{s_0 s_1}{s_0 + s_1} \quad \text{and} \quad L_{1,2} = \frac{s_0 (s_1 + s_2)}{s_0 + s_1 + s_2} \quad [\text{Koujournian74}].$$

However, in the slope diffraction method this analytical formula will not guarantee the continuity along the shadow boundary of all the diffracted waves, and therefore cannot be used to compute L for all diffracted waves. An example where a numerical evaluation of L is needed occurs in the case of three wedges: for the wave which is first diffracted at wedge1, then slope-diffracted at wedge2, and finally diffracted at wedge3. Only numerical enforcement, such as the one described here, will allow the correct computation of the distance factor at wedge3.

b) Similarly to step a) above, the continuity equation for the amplitude wave diffracted from wedge1 and reaching $SBP_{2,1}$ is:

$$0.5|E_I(SBP_{2,1})| = |E_2(SBP_{2,1})| \quad (3.a)$$

$$0.5|E_I(SBP_{2,1})| = |E_I(W_2) D_2(SBP_{2,1})| A_2(s_2) \quad (3.b)$$

$$|E_I(SBP_{2,1})| = |E_I(W_2)| \sqrt{L_{2,1}} A_2(s_2) \quad (3.c)$$

The computation of $E_I(SBP_{2,1})$ and $E_I(W_2)$ in (3) requires $L_{1,1}$ and $L_{1,2}$ which are now known from step a) above. Thus equ. (3) will allow the computation of $L_{2,1}$ needed to compute the double diffracted ray reaching the receiver.

c) The continuity equation for the slope of the wave diffracted from wedge1 and reaching $SBP_{2,1}$ is:

$$0.5 \left| \frac{\partial E_I(SBP_{2,1})}{\partial n} \right| = \left| \frac{\partial E_I(W_2)}{\partial n} \right| \frac{\partial D_2^s(SBP_{2,1})}{\partial n} |A_2(s_2)| \quad (4.a)$$

$$\left| \frac{\partial E_I(SBP_{2,1})}{\partial n} \right| = \left| \frac{\partial E_I(W_2)}{\partial n} \right| L_{s2,1}^{3/2} A_2(s_2) \quad (4.b)$$

where: $L_{S_{i,k}}$ is the distance factor used in the computation of the slope-diffraction from wedge i to $SBP_{i,k}$

Equ. (4) expresses the fact that at the shadow boundary the slope of the slope-diffracted wave ($\frac{\partial E_1(W_2)}{\partial n} \frac{\partial D_2^s}{\partial n} / A_2(s_2)$) is one-half the slope of the diffracted field ($\frac{\partial E_1(SBP_{2,1})}{\partial n}$). The

substitution in equ. (4.a) of $|\frac{\partial D_2^s(SBP_{2,1})}{\partial n}|$ by $0.5 L_{S_{2,1}}^{3/2}$ was

explained in the case of an absorbing edge in [Andersen97]. This substitution holds also for a conducting knife edge or for the more general surface impedance wedge, for the same reasons explained under a).

The algorithm applied for the case of two diffractions can be generalized to an arbitrary configuration of wedges or edges. Thus, starting from the wave radiated by the source, and then for each diffracted (slope-diffracted) wave the continuity equation of the amplitude (slope) of the wave in consideration must be imposed on all the shadow boundary points of the wedges on which the wave considered is incident. These continuity equations will allow determination of all the L and L_s factors needed in the computations of the diffracted and slope-diffracted waves reaching the receiver.

Note that in general it is not possible to enforce the continuity along the shadow boundaries of the diffracted and slope diffracted fields and their first-order derivatives in both magnitude and phase using real L-values. It was found that enforcing the continuity of the diffracted and slope diffracted fields and their first-order derivative in both magnitude and phase is only possible if all the edges and the transmitter lie exactly on the shadow boundary. That is why in equ. 2, 3 and 4 continuity is limited to the absolute values. This was sufficient in all the examples shown letter.

III. VALIDATION AGAINST PUBLISHED RESULTS

Andersen's method is an heuristic extension of the classical UTD, and no general proof is available to demonstrate that this extension is, in general, an accurate approximation of the exact solution. As for the UTD, only agreement with known solutions at various special configurations provides evidence about the validity of Andersen's method. Andersen provided such evidence for some absorbing screen configurations. In [Andersen97] however no validation of the method was given for wedge configurations. Multiple diffraction by wedges deserves particular attention as Andersen's method is among few schemes available in the literature that can handle multiple diffraction in transition region by wedges. Therefore, Andersen's method was implemented for wedge configurations and validated against published results in two wedge configurations. In addition, two of

the absorbing screen geometries in [Andersen97] are computed in this section.

A) Example 1: screens of equal height and equal spacing

The slope diffraction method is applied to the canonical multiple diffraction over screens of equal height and equal spacing shown in Figure 2. The slope diffraction method shows an error of less than one dB when compared to the exact solution [Lee78, Vogler82] after 10 diffractions. After 10 screens the method diverges from the exact solution, leading to a 3 dB overestimation of the received power after 14 screens. However, in all cases the slope diffraction method improved dramatically the accuracy of the classical UTD in this canonical example. Note that Vogler's method can only handle absorbing knife edge configurations and it is less computationally efficient than Andersen's method.

B) Example 2: screens of unequal height and unequal spacing

Figure 3 shows the slope diffraction computation for a 30-km propagation path ($f=100$ MHz). In the path there are two knife edges at distances 10 km and 20 km from the transmitter, each at a fixed height of 100 m. Both the transmitter and the receiver are at level 0. A third knife edge is placed in the middle of the path at a variable height h_2 . This configuration was computed in [Vogler82] using Vogler's exact solution. The slope diffraction results shown in Figure 3 are within 0.4 dB of the exact solution. In [Andersen97] the attenuation for the same example presented here is computed. Although not shown here, our computations were compared to the curves due to Vogler and Andersen. It was found: 1) The attenuation in [Andersen97] exhibits a first order discontinuity at the shadow boundary, i.e. at $h_2=100$ m, and 2) our computation is slightly more accurate than in [Andersen97] for unknown reasons that need to be clarified.

C) Example 3: Two perfectly conducting wedges with small interior angles

The slope diffraction method was also implemented for wedge configurations. The method was found to give accurate results when compared with some published results. Here we will show the results for a diffraction geometry involving two perfectly conducting wedges with interior angles of 60° . The results are in perfect agreement with the results shown in [Holm96]. The advantage of the slope diffraction method over the method presented in [Holm96] is that it requires only one higher-order term (the slope term) whereas the method in [Holm96] requires at least six. Therefore Holm's method is less computationally efficient than Andersen method.

D) Example 4: Two perfectly conducting wedges with large interior angles

Another example from [Holm96] involves the diffraction by two perfectly conducting wedges. Our computations shown in Figure 5 are in perfect agreement with Holm's computation. The difference with example 3 above, is that here we are in the

vicinity of the reflection boundaries. Therefore the diffraction by the two wedges cannot be approximated by edge diffractions. Holm states that for example 4 and 5, the wedges could be replaced by edges without any major difference in the diffraction loss. Although not shown here, our computations confirm this claim.

IV. IMPROVEMENT DUE TO THE SLOPE DIFFRACTION METHOD IN AN URBAN ENVIRONMENT

The shortcoming of the classical UTD [Kouyoumjian74] in the computation of multiple diffraction in the transition region was, in some published works [Maciel93], among the reasons for not using it in the prediction of propagation in the vertical plane. On the other hand when the classical UTD was used for the computation of multiple diffraction in the transition region as in [Kurner93] the inaccuracies of the method were not stated. As the classical UTD is faster and more simple to implement than the slope diffraction method, it is worthwhile to determine in which environments it is or is not accurate. It then becomes possible to make a tradeoff between accuracy and computation time and/or between accuracy and implementation complexity. To perform our study we make comparisons between the computations by the classical UTD and by the slope diffraction method, of multiple diffractions in the geometry shown in Figure 6. The geometry in Figure 6 includes 10 equally spaced screens with heights distributed according to a uniform distribution $U[18-\Delta h, 18+\Delta h]$ m. The transmitter is located at a height of 18 m.

The contribution of the slope diffraction to multiple diffraction depends mainly on the extent to which successive screens are located in the transition region of previous screens. Considering the notation in Figure 1, the equation of the transition region is [McNamara90, equ. 4.133]:

$$\frac{2s_0 s_1 \cos^2\left(\frac{\phi_1 - \phi_1'}{2}\right)}{\lambda(s_0 + s_1)} \leq 1 \quad (5)$$

Therefore the transition region depends on the separation between screens (d), the frequency (freq) and the difference in building heights (Δh). To perform a study that applies to a wide range of environments we will consider the following values for the three parameters freq , d , and Δh :

$$\text{freq: } 900, 1800 \text{ MHz; } d: 12.5, 25, 50\text{m; } \Delta h: 1, 3, 6, 9 \text{ m.}$$

Thus there are 32 different configurations to consider. However, freq , d and Δh do not influence the contribution of the slope diffraction in an independent manner. From simple geometrical considerations it can be shown that, for $d \gg \Delta h$ the left side in equ. (5) is proportional to the quantity: $\Delta h^2/(\lambda*d)$. Therefore, instead of analyzing the influence of freq , d and Δh independently, it is sufficient to analyze the influence of $\Delta h^2/(\lambda*d)$. The quantity $\Delta h^2/(\lambda*d)$ will be called *Transition Region Width TRW*. To verify that TRW is sufficient to describe the influence of freq , d and Δh on the contribution of the slope

diffraction, the following test was performed: we computed the error $\text{Err}_{\text{UTD-Slope}}$ between the received power computed with and without the slope diffraction for three sets of values, freq [MHz], d [m] and Δh [m]: {900, 100, 3}, {450, 50, 3} and {900, 50, $3/\sqrt{2}$ }. It was verified that the three configurations lead to similar $\text{Err}_{\text{UTD-Slope}}$ for all realizations (within less than 0.2 dB in most realizations).

Table 1 gives the TRW values for all the environment configurations we shall study in this section. From Table 1 it is seen that 8 values of TRW are representative of all the variations in the frequency, the average separation between screens, and the deviations between screen heights.

Table 1 Transition Region Width (TRW) for several values of screen separation (d) and standard deviation of screen heights ($2s$) at frequency 900 MHz. The values in brackets correspond to frequency 1800 MHz

Δh [m]	1	3	6	9
d [m]				
12.5	.24 (.48)	2.16 (4.32)	8.64 (17.28)	19.44 (38.88)
25	.12 (.24)	1.08 (2.16)	4.32 (8.64)	9.72 (19.44)
50	.06 (.12)	.54 (1.08)	2.16 (4.32)	4.86 (9.72)

In Table 2 the 8 relevant values of TRW retained from Table 1 are listed in the first column, along with the average error (η) and the standard deviation (σ) of $\text{Err}_{\text{UTD-Slope}}$ for 25 realizations of the geometry shown in Figure 6. We considered two types of the classical UTD computations: 1) computations using the phase summing of the received rays, and 2) the computations using the power summing of the rays. In the slope diffraction method the received rays are summed in phase. It is worth noting here that for $\text{TRW} < 4$ it can be shown that all the screens are in the transition regions of all the others.

Table 2 with average error (η) and the standard deviation (σ) of $\text{Err}_{\text{UTD-Slope}}$ for 10 realizations of the geometry shown in Figure 6

Transition Region Width TRW	Error between Slope diffraction and classical UTD (phase summing)		Error between Slope diffraction and classical UTD (power summing)	
	η [dB]	σ [dB]	η [dB]	σ [dB]
0	-40	0	-40*	0
0.06	-6.0	4.0	3.9	6.8
0.24	-5.6	3.5	2.8	4.3
0.54	-4.5	3.0	1.7	4.7
1.08	-4.0	3.4	1.6	4.3
2.16	-2.6	2.1	1.3	4.3
4.32	-2.2	2.4	1.6	3.8
9.72	-1.4	1.5	1.6	3.4

* When $\text{TRW}=0$ $\Delta h = 0$, i.e. all the edges are at the same height. It was assumed that only one ray exists in this case. Therefore phase summing results are identical to power summing results

From Table 2 the following observations can be made:

- 1- In spite of the fact that in most of the configurations considered, all screens are in the transition regions of all others, the improvement due to the slope diffraction method

Published in the Proceedings of the IEEE 48th Vehicular Technology Conference

never exceeds 6 dB, except in the canonical geometry of 10 screens of equal height and equal spacing ($TRW = 0$).

- 2- for $TRW \geq 1$ ($\{freq = 1800MHz, d=50m, \Delta h=3m\}$ or $\{freq = 1800MHz, d=25m, \Delta h=2m\}$) the classical UTD used in conjunction with power summing is within an average value of 1.6 dB from the slope diffraction method. This opens the door to the use of the classical UTD in environments where it was usually not considered to be valid

The relatively low error of the classical UTD when the screens are not exactly at the shadow boundary can be explained by looking at figure 4 in [Holm96]. The author compared the classical UTD and the exact solution for example 2 above (sect. III). The middle screen starts to penetrate the transition region at a height equal to -112 m. However, the error between the exact solution and classical UTD remains constant until the middle screen reaches a height of approximately 90 m. Thus the error becomes noticeable only when the middle screen penetrates about 90% of the transition region area. Considering an example of two screens as in Figure 1 at a frequency of 900 MHz and $s_0=s_1=50m$, a 90% penetration of wedge2 in the transition region of wedge1 means that wedge2 is located at 0.8 m from the shadow boundary.

V. CONCLUSIONS

In this paper we described an algorithm for the implementation of the innovative concept of the slope diffraction as presented in [Andersen97], for an arbitrary configuration including edges or wedges. Validation against several published results was presented. The validations include examples of wedge configurations for which no validation of the slope diffraction method is available in the literature.

Furthermore, we performed an estimation, for an urban environment, of the improvement due to the use of the slope diffraction method over the classical implementation of UTD. The amount of improvement obtained due to the slope diffraction versus the classical UTD in an urban environment was found to be directly related to a factor we called the *Transition Region Width* TRW. Based on the equation of the transition region, TRW relates the three parameters influencing the slope diffraction contribution (the frequency $freq$, the separation between two screens d , and difference in screen heights Δh) into one parameter: $\Delta h^2/(\lambda*d)$. We found that:

- for $TRW \geq 1$, which corresponds for instance to $\{freq = 1800MHz, d=50m, \Delta h=3m\}$ or $\{freq = 1800MHz, d=25m, \Delta h=2m\}$, the classical UTD used in conjunction with a power summing of rays leads to similar results (within ~1.6 dB) as the slope diffraction method. The results were obtained from 25 realizations of 10 equally spaced screens with heights distributed according to a uniform distribution $U[18-\Delta h, 18+\Delta h]$ m. These findings open the door for to use of the classical UTD in environments where it was usually considered not to be valid. The classical UTD is faster and

simpler to implement than the slope diffraction method. Further investigation is needed to determine to what extent these findings remain valid for a larger number of screens.

- for $TRW < 1$, the error between the received power, with and without the slope diffraction contribution, increases to reach an average value of 6 dB and a standard deviation of 6 dB for $TRW = 0.1$, which corresponds for instance to $\{freq = 900MHz, d=50m, \Delta h=1m\}$.

To the best of our knowledge this is the first time where an evaluation is performed for the error due to the use of the classical UTD for the computation of multiple transition region diffractions for screens with unequal heights such as in an urban or suburban environment. Before performing this comparison we expected that the inaccuracies of the classical UTD would be higher. Further investigation is needed to determine the extent to which these findings are valid for a larger number of screens.

ACKNOWLEDGMENT

The proficient help and assistance of Dr. S. Fortune of Bell Labs in the aspects related to the WiSE tool were specially appreciated. The stimulating discussions held with Prof. J. B. Andersen and Dr. M. Gans of Bell Labs were especially valuable, and are gratefully acknowledged.

REFERENCES

- Andersen, J. B., "UTD transition region diffraction," *IEEE Trans. Antennas Propag* 1997
- Groskopf, R., "Comparison of different methods for the prediction of the field strength in VHF range," *IEEE Trans. Antennas Propag.*, vol. AP-35, no. 7, pp. 852-859, July 1987.
- Hata, M., "Empirical formula for propagation loss in land mobile radio services", *IEEE Trans. on Vehicular Technology*, Vol. 29, 1980, 317-325.
- Holm P. D., "UTD-diffraction coefficients for higher order wedge diffracted fields," *IEEE Trans. Antennas Propag.*, vol. AP-44, no. 6, pp. 879-888, 1996.
- Kouyoumjian R. G. and P. H. Pathak, "A uniform geometrical theory of diffraction for an edge in a perfectly conducting surface", *Proc. IEEE*, pp. 1448-1468, Nov. 1974.
- Kurner T., D. Cichon, and W. Wiesbeck, "Concepts and results for 3D digital terrain-based wave propagation models: an overview", *IEEE Journal Slect. Areas Comm.*, vol. 11, no 7, Sept. 1993
- Lachat E., J. F. Wagen, and J. Li, "Effects of building heights on predictions in Munich using a multiple vertical-knife-edges propagation model," *Proceedings IEEE 47th Vehicular Technology Conference*, pp. 261-265, Phoenix, USA, May 1997.
- Lee S. W. and J. Boersma, "Ray-optical analysis of fields on shadow boundaries of two parallel plates," *J. Math. Phys.*, vol. 16, 1978, pp. 1746-1764
- Li J., J. F. Wagen, and E. Lachat, "Propagation over rooftop and in the horizontal plane for small and micro-cell coverage predictions," *Proceedings IEEE 47th Vehicular Technology Conference*, pp. 1123-1127, Phoenix, USA, May 1997.
- Maciel L. R., H. L. Bertoni, and H. H. Xia, "Unified approach to prediction of propagation over building for all ranges of base station

Published in the Proceedings of the IEEE 48th Vehicular Technology Conference

antenna height," *IEEE Trans Vehicular Tech.*, VT (42), no. 1, Feb. 1993.

McNamara D. A., C. W. I. Pistorius and J. A. G. Malherbe, "Introduction to the uniform geometrical theory of diffraction", *Artech House*, 1990

Saunders S. R. and F. R. Bonar, "Explicit multiple building diffraction attenuation function for mobile radio wave propagation," *IEE Electronic Letters*, vol 27, no 14, pp. 1276-1277, Jul 1991

Vogler L., "An attenuation function for multiple knife-edge diffraction," *Radio Science*, 17, pp. 1541-1546, 1982

Walfisch J., and H. L. Bertoni, "A theoretical model of UHF propagation in urban environments," *IEEE Trans. Antennas Propag.*, vol. AP-36, no. 12, pp. 1788-1796, Dec. 1988

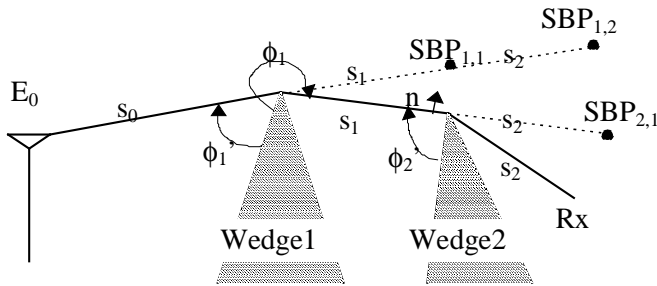


Figure 1 Geometry and notation. To a wedge i correspond $(n-i+1)$ Shadow Boundary Points (SBP), where n is the total number of wedge

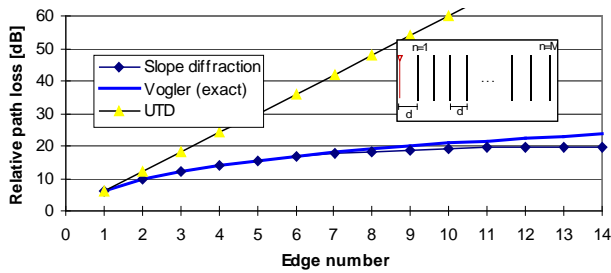


Figure 2 Path loss relative to the direct loss versus knife edge number

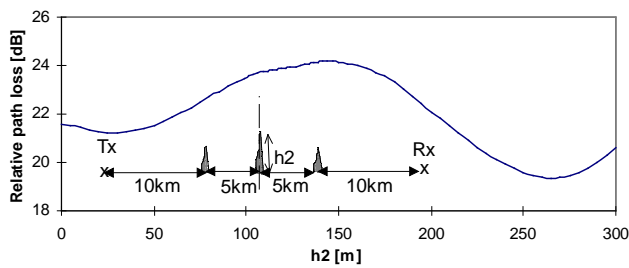


Figure 3 Path loss relative to the direct loss versus knife-edge height h_2

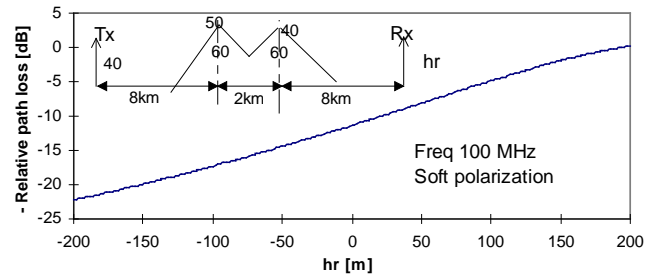


Figure 4 Path loss relative to the direct loss versus receiver height h_r , for two perfectly conducting wedges

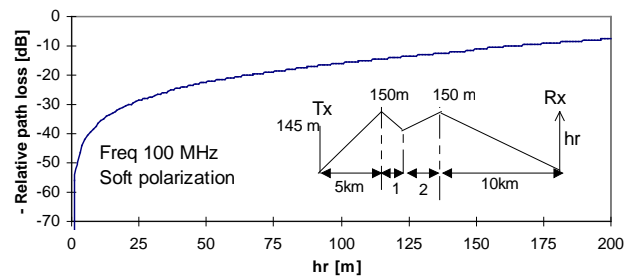


Figure 5 Path loss relative to the direct loss versus receiver height h_r for two perfectly conducting wedges

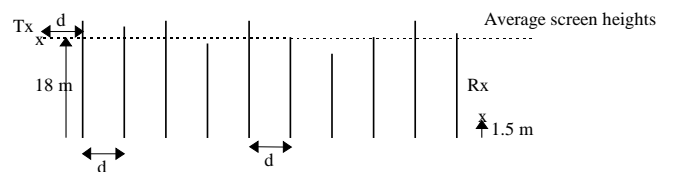


Figure 6 equally spaced screens with heights distributed according to a uniform distribution $U[18-\Delta h, 18+\Delta h]$ m